

Orientation Effects in Triplet–Singlet Difference Spectroscopy Measured with Absorbance-Detected Magnetic Resonance[†]

Gabrielle M. Owen and Arnold J. Hoff^{*,‡}

Department of Biophysics, Huygens Laboratory, Leiden University, P.O. Box 9504,
2300 RA Leiden, The Netherlands

Received: October 5, 1999

Absorbance-detected magnetic resonance (ADMR) triplet–singlet difference (T–S) spectra are often measured with unpolarized light. We show that under nonsaturating conditions ADMR spectra are a function of the angles between the optical and microwave transition moments. T–S spectra measured in this manner are not in agreement with the widely accepted definition of T–S spectra as the angle-independent difference between triplet and singlet absorbance. In order to remove the dependence on the angle between the transition moments from the ADMR-detected T–S spectra, T–S spectra have been recorded as the sum of the change in absorbance with light polarized parallel plus twice the change in absorbance with light polarized perpendicular to the microwave field. Spectra are shown for the photosynthetic bacterium *Rhodobacter sphaeroides* R26 and the Fenna–Matthews–Olson (FMO) complex of the green sulfur bacterium *Prosthecochloris (Pr.) aestuarii*.

1. Introduction

In optically-detected magnetic resonance (ODMR) spectroscopy the changes in an optical property (absorbance, fluorescence, or phosphorescence) induced by a microwave field resonant with two sublevels of the triplet state are measured.^{1,2} With absorbance-detected magnetic resonance (ADMR) the change in absorbance is detected with and without a microwave field that is resonant with a zero-field transition of the triplet sublevels. For the biological systems under consideration in this paper, the incident light can induce a singlet–singlet ($S_1 \leftarrow S_0$) transition or a triplet–triplet ($T_1 \leftarrow T_0$) transition. The change in absorption can also be monitored at one wavelength as a function of the microwave frequency.

The former technique is known as triplet–singlet difference (T–S) spectroscopy² or microwave-induced absorbance (MIA).³ When the difference in absorbance is measured with linearly polarized light, the resulting linear-dichroic ADMR or LD(T–S) spectra reveal information about the angles α between the optical transition dipole moment of either the triplet or the singlet transition and the magnetic transition dipole moment of the zero-field transition. These angles reveal information about the triplet state present in the system and are inaccessible by conventional absorbance, LD, or circular dichroism (CD) spectroscopy.

T–S and LD(T–S) spectra have been recorded for a wide variety of biological, photosynthetic systems. The angle between the optical transition moment of the singlet or triplet state and the microwave transition moment of the triplet has been elucidated for each band in the absorption spectrum.^{4–8} Also, the ADMR spectra have been used in combination with other optical spectra in exciton simulations of photosynthetic complexes.^{9–12} In these references unpolarized light was used, and the presented T–S spectra were detected in three possible

ways: with no polarizer, a combination of a photoelastic modulator and polarizer, or only a polarizer. In the first two methods the sum of the absorption of light with the polarization parallel (ΔA_V) and perpendicular (ΔA_H) to the polarization of the microwave field is measured, and in the third method, ΔA_V and ΔA_H are independently recorded. These three ways of measuring T–S spectra are equivalent ways of measuring ($\Delta A_V + \Delta A_H$), as is shown with Stokes-Mueller matrices in ref 13. The T–S spectra measured under nonsaturating conditions, however, are a function of the angle α itself. This fact is inconsistent with the widely accepted definition of T–S spectra as the difference between the α -independent, isotropic triplet and singlet absorbances.

In the present article we derive new formulas for the changes in absorption of the system with the incident light polarized parallel and perpendicular to the polarization of the microwave field. We use them to show that T–S spectra can be made independent of α when presented as the sum of the change in absorption with light polarized parallel plus *twice* the change in absorption with light polarized perpendicular to the polarization of the microwave field ($\Delta A_V + 2\Delta A_H$). We present α -dependent and α -independent T–S spectra and LD(T–S) spectra for reaction centers (RCs) of the photosynthetic bacterium *Rhodobacter (Rb.) sphaeroides* R26 and for the Fenna–Matthews–Olson (FMO) complex of the green sulfur bacterium *Prosthecochloris (Pr.) aestuarii*, and we show that previous results for these complexes should be reconsidered.

2. Polarized Spectroscopy with ADMR

In this section we explain the basic principles of ADMR spectroscopy and derive formulas that describe the change in absorbance of light polarized perpendicular ($\Delta A_H(\lambda)$) or parallel ($\Delta A_V(\lambda)$) to the microwave field. The change in absorbance $\Delta A_e(\lambda)$ of light with the polarization of the electric field in the direction \hat{e} (where \hat{e} denotes a unit vector) for an ensemble of N coupled pigments is found by first finding the probability that an excited pigment at a particular orientation with respect to the polarization of the microwave field makes a microwave

[†] Abbreviations: ODMR, optically-detected magnetic resonance; ADMR absorbance-detected magnetic resonance; MIA, microwave-induced absorbance; T–S, triplet minus singlet; LD, linear dichroism; CD, circular dichroism; RC, reaction center; FMO, Fenna–Matthews–Olson complex.

[‡] Telephone: +31 71 5275955. Fax: +31 71 5275819. E-mail: hoff@biophys.LeidenUniv.NL.

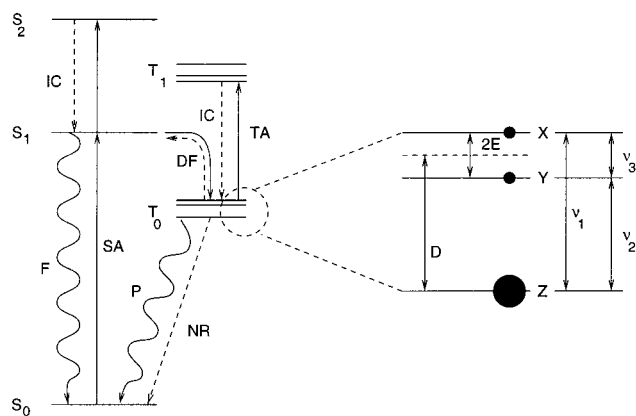


Figure 1. Energy level diagram of the singlet and triplet manifold: S_0 , singlet ground state; S_1 and S_2 , singlet excited states; T_0 and T_1 , first and second excited triplet states; SA and TA, singlet and triplet absorption, respectively; F and DF, fluorescence and delayed fluorescence, respectively; P, phosphorescence; NR, nonradiative transition; IC, internal conversion. Enlarged T_0 levels: X, Y, and Z, eigenenergies of the dipole–dipole interaction; D and E , zero-field splitting parameters. Filled circles: equilibrium populations. ν_1 , ν_2 , and ν_3 are the frequencies corresponding to the $(|D| \pm |E|)/h$ and $2|E|/h$ transitions, respectively.

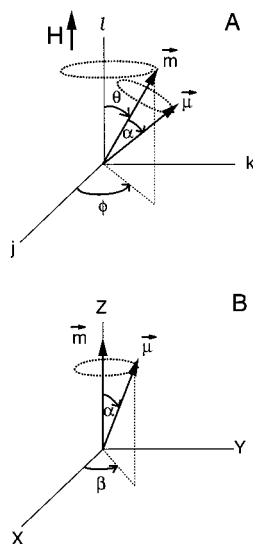


Figure 2. (A) Magnetic \vec{m} and optical $\vec{\mu}$ transition moments in the laboratory axis system (jkl). The vector \vec{m} lies at an angle θ from the \hat{l} axis, which is the direction of the polarization of the magnetic field \vec{H} . The projection of \vec{m} on the j – k plane is at an angle ϕ from the j -axis. (B) Position of \vec{m} and $\vec{\mu}$ in the triplet axis system (xyz). The vector $\vec{\mu}$ lies at an angle α from \vec{m} , and the projection of $\vec{\mu}$ on the x – y plane lies at an angle β from the x -axis.

transition. This probability is then multiplied by the extinction coefficient corresponding to the optical transition, and the result is summed over all possible orientations of the molecule.

A general energy-level scheme for the singlet (S) and triplet (T) state of one pigment is shown in Figure 1. In the enlarged section the three triplet sublevels (X, Y, Z) of the lowest triplet state T_0 are visible along with the zero-field-splitting (zfs-) parameters D and E , which are customarily used to express the energy differences between the sublevels. For a zero-field transition to occur, the microwave frequency should be resonant, and the polarization of the microwaves should have a component parallel to the microwave transition moment \vec{m} . The vector \vec{m} is specified by the angles θ and ϕ in the laboratory axis system jkl , as shown in Figure 2A. The microwave field is polarized in the direction \hat{l} , and the light propagates in the direction \hat{k} (\hat{k}

$\perp \hat{e}$). Transitions between S_0 and higher singlet states, or between T_0 and higher triplet states occur when the frequency of the light is tuned to resonance and when the polarization of the light has a component parallel to the electric transition dipole $\vec{\mu}$. In the triplet axes system xyz , $\vec{\mu}$ is described as

$$\vec{\mu}(\alpha, \beta) = |\mu| \begin{vmatrix} \cos \beta \sin \alpha \\ \sin \beta \sin \alpha \\ \cos \alpha \end{vmatrix} \quad (1)$$

where α and β are polar angles (see Figure 2B).

During steady-state illumination, the sum of the concentration of pigment complexes in the lowest singlet and triplet state, $[S_0] + [T_0]$, is constant. Under the assumption that the higher excited singlet and triplet states are unpopulated because of their short lifetimes, the change in $[S_0]$ during application of a resonant magnetic field is equal in magnitude and opposite in sign to the change in $[T_0]$. The change in absorbance $\Delta A_e(\lambda)$ with the microwave field turned on is given by ref 14 and the Beer–Lambert law:¹⁵

$$\Delta A_e(\lambda) = -2.303l[\Delta S_0]\{\epsilon_S(\lambda) - \epsilon_T(\lambda) - \epsilon_{ST}(\lambda)\} \quad (2)$$

Here l is the thickness of the sample and, for a system of coupled molecules, $\epsilon_S(\lambda)$ is the extinction coefficient for all singlet–singlet ($S_1 \leftarrow S_0$) absorbances with no pigments in the triplet state, $\epsilon_T(\lambda)$ is the extinction coefficient for all triplet–triplet ($T_1 \leftarrow T_0$) absorbances in the triplet state T_0 , and $\epsilon_{ST}(\lambda)$ is the extinction coefficient for all $S_1 \leftarrow S_0$ absorbances with another pigment already in the triplet state.

In eq 2, $[\Delta S_0]$ is proportional to the probability $p(\theta, \phi)$ that a molecule with its microwave transition moment specified by the angles (θ, ϕ) has made a microwave transition.¹⁵ This probability is given by

$$p(\theta, \phi) = \frac{\pi}{4} \frac{|V_m(\theta, \phi)|^2}{\hbar^2} \delta((\omega_m - \omega)/2) \quad (3)$$

where $V_m(\theta, \phi)$ is the time-independent part of the interaction Hamiltonian, δ is the delta function, ω_m is the frequency difference between two T_0 sublevels, and ω is the frequency of the microwave field. When a microwave field with polarization \hat{l} and amplitude H is used below saturating power, the interaction is given by $V_m(\theta, \phi) = -|H||m| \cos \theta$,¹⁵ where θ is the angle between \vec{m} and \hat{l} (see Figure 2A). The fraction of excited molecules $P(\theta, \phi)$ is

$$P(\theta, \phi) = \frac{p(\theta, \phi)}{\int_{\phi=0}^{2\pi} \int_{\theta=0}^{\pi} p(\theta, \phi) \sin \theta d\theta d\phi} = \frac{c_T \cos^2 \theta}{\int_{\phi=0}^{2\pi} \int_{\theta=0}^{\pi} c_T \cos^2 \theta \sin \theta d\theta d\phi} \quad (4)$$

with $c_T = [\pi l / 4 \hbar^2] |Hm|^2 \delta((\omega_m - \omega)/2)$.

For the optical transition, the extinction coefficient ϵ is defined as¹⁵

$$\epsilon = \frac{N}{2303} \frac{w}{I} \quad (5)$$

where N is Avogadro's number, I is the intensity of the incident light ($\text{erg cm}^{-2} \text{s}^{-1}$), and w is the average energy absorbed per molecule per second for the electronic transition. For an $S_1 \leftarrow S_0$ or $T_1 \leftarrow T_0$ transition, $w(\omega_\lambda, \alpha, \beta)$ is

$$w(\omega_\lambda, \alpha, \beta) = \frac{\pi\omega_\lambda |V_o(\alpha, \beta)|^2 \rho(\omega_\lambda)}{2\hbar} \quad (6)$$

where $\rho(\omega_\lambda)$ is a line-shape factor, ω_λ is the frequency of the light, and $V_o(\alpha, \beta)$ is the time-independent part of the Hamiltonian. For light with electric field of amplitude E_o and polarization \hat{e} , $V_o(\alpha, \beta) = -E_o \hat{e} \cdot \vec{\mu}(\alpha, \beta)$.¹⁵

The change in absorbance in eq 2 is proportional to the sum of three ϵ terms. For one ϵ term the infinitesimal change in absorbance at wavelength λ , $\delta A_e(\lambda)$, caused by a pigment–protein complex with an orientation (θ, ϕ, β) (see Figure 2), is found by using eqs 2 and 4–6 and summing over all N pigments:

$$\delta A(\lambda)_e \propto \sum_{i=1}^N |\hat{e} \cdot \vec{\mu}_i(\alpha, \beta)|^2 \rho_i(\omega_\lambda) P(\theta, \phi) \quad (7)$$

In order to calculate the change in absorbance $\Delta A_e(\lambda)$, eq 7 has to be integrated over all possible orientations of the system. In the laboratory axes system, the excited optical transitions $\vec{\mu}(\alpha, \beta)$ form the surface of a cone with angle α around the microwave transition \vec{m} , as shown in Figure 2. Similarly the excited magnetic moments lie on the surface of a cone with angle θ around the polarization of the magnetic field (Figure 2A). The quantity $\Delta A_e(\lambda)$, corresponding to the ϵ_S , ϵ_T , or ϵ_ϵ is

$$\Delta A_e(\lambda) \propto \sum_{i=1}^N \int_{\phi=0}^{2\pi} \int_{\theta=0}^{\pi} \int_{\beta=0}^{2\pi} (\hat{e} \cdot (\mathbf{R}_\phi \cdot \mathbf{R}_\theta \cdot \vec{\mu}_i(\alpha, \beta)))^2 \rho_i(\omega_\lambda) P(\theta, \phi) \sin \theta_i d\beta d\theta d\phi \quad (8)$$

where \mathbf{R}_ϕ and \mathbf{R}_θ are matrices which rotate $\vec{\mu}$ over θ and ϕ with respect to the laboratory l and j axis, respectively. The change in absorption at wavelength λ with the electric field polarized parallel ($\Delta A_V(\lambda)$) and perpendicular ($\Delta A_H(\lambda)$) to the polarization of the microwave field is calculated from eq 8:

$$\Delta A_V(\lambda) = \Delta A_l(\lambda) = \frac{1}{5} \sum_{i=1}^N \mu_i^2 \rho_i(\omega_\lambda) (1 + 2 \cos^2 \alpha_i) \quad (9)$$

$$\Delta A_H(\lambda) = \Delta A_j(\lambda) = \frac{1}{5} \sum_{i=1}^N \mu_i^2 \rho_i(\omega_\lambda) (2 - \cos^2 \alpha_i) \quad (10)$$

As is seen from eqs 9 and 10, the quantity $\Delta A(\lambda) = \Delta A_V(\lambda) + 2\Delta A_H(\lambda)$ is independent of α . The expressions for the change in absorption for the T–S and LD(T–S) experiment are obtained from eqs 2, 9, and 10:

$$\Delta A_{T-S}(\lambda) = \Delta A_V(\lambda) + 2\Delta A_H(\lambda) \quad (11)$$

$$= \sum_{i=1}^N [|\mu_{Si}|^2 \rho_i(\omega_\lambda) + |\mu_{Ti}|^2 \rho_i(\omega_\lambda) - |\mu_{Si}|^2 \rho_i(\omega_\lambda)] \quad (12)$$

$$\Delta A_{LD(T-S)}(\lambda) = \Delta A_V(\lambda) - \Delta A_H(\lambda) \quad (13)$$

$$= \frac{1}{5} \sum_{i=1}^N [|\mu_{Si}|^2 \rho_i(\omega_\lambda) (3 \cos^2 (\alpha_{Si}) - 1) + |\mu_{Ti}|^2 \rho_i(\omega_\lambda) (3 \cos^2 \alpha_{Ti} - 1) - |\mu_{Si}|^2 \rho_i(\omega_\lambda) (3 \cos^2 \alpha_{Si} - 1)] \quad (14)$$

where $|\mu_{Si}|$ and $|\mu_{Ti}|$ are the magnitudes of the dipole moments of the $S_1 \leftarrow S_0$ transition with or without a pigment in the triplet, respectively, and $|\mu_{Ti}|$ is the magnitude of the dipole moment of the $T_1 \leftarrow T_0$ transition. The angles between the optical and microwave transition moments for μ_{Si} , μ_{Ti} , and μ_{Ti} are α_{Si} , α_{Ti} , and α_{Ti} , respectively.

The (T–S)(α) spectra measured under nonsaturating conditions are dependent on the angles α . We will use the notation $\Delta A_{(T-S)(\alpha)}(\lambda)$ for the change in absorbance in the (T–S)(α) spectra. This change in absorbance is given by eqs 2, 9, and 10:

$$\Delta A_{(T-S)(\alpha)}(\lambda) = \Delta A_V(\lambda) + \Delta A_H(\lambda) \quad (15)$$

$$= \frac{3}{5} \Delta A_{T-S}(\lambda) + \frac{1}{5} \sum_{i=1}^N \times \{ |\mu_{Si}|^2 \rho_i(\omega_\lambda) \cos^2 \alpha_{Si} + |\mu_{Ti}|^2 \rho_i(\omega_\lambda) \cos^2 \alpha_{Ti} - |\mu_{Si}|^2 \rho_i(\omega_\lambda) \cos^2 \alpha_{Si} \} \quad (16)$$

which differs from $\Delta A_{T-S}(\lambda)$ (see eq 12) in the $|\mu|^2 \rho(\omega_\lambda) \cos^2 \alpha$ terms. The (T–S)(α) and the LD(T–S) data can be used to construct the α -independent T–S spectra. From eqs 12, 14, and 16, it follows that α -independent T–S spectra are given by

$$\Delta A_{T-S}(\lambda) = \frac{3}{2} \Delta A_{(T-S)(\alpha)}(\lambda) - \frac{1}{2} \Delta A_{LD(T-S)}(\lambda) \quad (17)$$

The shape of the T–S and (T–S)(α) spectra differs only if the LD(T–S) signal is sizable.

3. Results and Discussion

In this section we will present T–S spectra measured as $\Delta A_V + \Delta A_H$ and as $\Delta A_V + 2\Delta A_H$, from here on called (T–S)(α) and T–S spectra, respectively, for the reaction centers (RCs) of the photosynthetic bacterium *Rb. sphaeroides* R26 and for the FMO complex of *Pr. aestuarii*. For both systems, we will discuss the differences between the two types of spectra.

In RCs where forward electron transport is blocked, recombination of photoinduced charges gives rise to the triplet state of the primary donor *P*, a bacteriochlorophyll (BChl) dimer. In Figure 3A,B (T–S)(α) spectra (solid lines) are shown for RCs of *Rb. sphaeroides* R26 (data from ref 7) along with the α -independent T–S spectra (dotted lines) reconstructed from the data of ref 7 and eq 17. Figure 3A contains the spectra with the microwave frequency tuned to the $|D| - |E|$ transition of 3P . Figure 3B contains those with the microwave frequency tuned to the $|D| + |E|$ transition. In the 750–760 nm region bacteriopheophytins absorb.¹⁶ In the 790–820 nm region, accessory BChls and the symmetric component of the excitonically coupled BChl dimer absorb. The 900 nm band is assigned to the antisymmetric combination of the excitonically coupled BChl dimer (the P(–) band).^{6,10,17–19} The latter band is well separated from the spectral region of the accessory BChls.¹⁰

Insight into the saturation of the microwave transition is obtained by comparing the amplitude of the bands in the LD(T–S) spectrum to those in the (T–S)(α) spectrum. The LD(T–S) spectra (solid lines) measured as $(\Delta A_V - \Delta A_H)$ for the $|D| - |E|$ and $|D| + |E|$ transitions are shown in Figure 3C,D, respectively. For the $|D| - |E|$ transition the ratio of the LD(T–S) to the (T–S)(α) signal is approximately 0.5 at 808 nm, 0 at 818 nm, and 0.4 at 900 nm. For the $|D| + |E|$ transition the ratio of the LD(T–S) to the (T–S)(α) signal is ap-

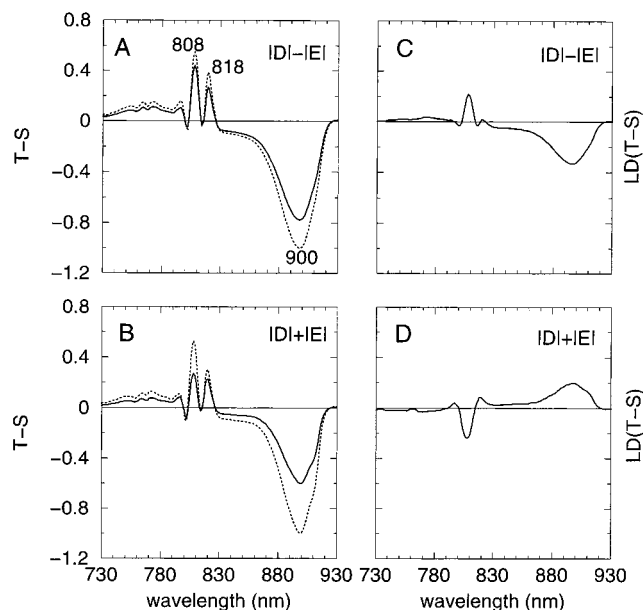


Figure 3. Microwave-induced (T-S)(α) absorbance difference spectra (solid line) and the T-S absorbance difference spectra (dotted line) of *Rb. sphaeroides* R26 reaction centers are shown in (A) for the $|D| - |E|$ transition (467 MHz) and in (B) for the $|D| + |E|$ transition (658 MHz). The LD(T-S) spectra measured as $(\Delta A_V - \Delta A_H)$ (solid line) are shown in (C) for the $|D| - |E|$ transition (467 MHz) and in (D) for the $|D| + |E|$ transition (658 MHz). The microwaves were amplitude modulated at 312 Hz. The optical resolution was set at 3 nm. The subscripts V and H refer to parallel and perpendicular to the direction of the microwave magnetic field. The extrema (in nm) in the T-S spectra are indicated in (A) and also hold for (B)–(D). The y-axis labels for the T-S spectra also hold for the LD(T-S) spectra of the same microwave transition. Data are from ref 7.

proximately -0.9 at 808 nm, 0.4 at 818 nm, and -0.3 at 900 nm. The magnitude of this ratio is much larger than zero for both transitions. If the microwave transition is saturated, $P(\theta, \phi)$ is independent of θ and ϕ , and there will be no difference in the absorption of light polarized parallel or perpendicular to the polarization of the magnetic field. The observation of a sizable LD(T-S) signal indicates that the microwave transition is not saturated in these experiments.

When a (T-S)(α) spectrum measured under nonsaturating conditions is incorrectly characterized with eq 11 as a T-S spectrum, erroneous information about the angles α is extracted from the spectrum. Especially the exciton simulations are susceptible to errors because *both* the amplitudes and line shapes are modeled. For example, the relative distances, orientations, and magnitudes of the dipole moments derived from exciton simulations that simultaneously fit several sets of optical data^{8,9,20} should be reconsidered when a (T-S)(α) spectrum measured under nonsaturating conditions is treated as a T-S spectrum.

We first address the differences in shape between T-S spectra measured in the two manners. In Figure 4A the (T-S)(α) spectrum (solid line) and the T-S spectrum (dotted line) for the $|D| - |E|$ transition are shown, where the spectra are scaled such that the overlap is maximum. The spectra are nearly identical except for small differences (dashed line) in the accessory BChl region. In Figure 4B the spectra for the $|D| + |E|$ transition are shown. The differences in the accessory BChl region are larger than those for the $|D| - |E|$ but are still small. The sum of $|\mu|^2 \rho(\omega_i) \cos^2 \alpha$ terms in eq 16 is evidently small for reaction centers of *Rb. sphaeroides* because of overlapping bands with nearly identical angles α and a value of α close to 90° for the P(–) band in the spectrum of Figure 4B. The

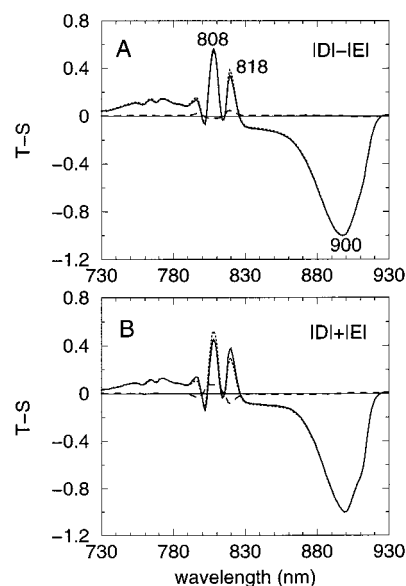


Figure 4. The microwave-induced (T-S)(α) absorbance difference spectra (solid line) and the T-S absorbance difference spectra (dotted line) of *Rb. sphaeroides* R26 reaction centers are shown in (A) for the $|D| - |E|$ transition (467 MHz) and in (B) for the $|D| + |E|$ transition (658 MHz). The spectra are scaled so that the overlap is maximal. The difference between the (T-S)(α) spectra and the T-S spectra is shown with a dashed line. The measuring conditions were the same as in Figure 3. Data are from ref 7.

differences between the amplitudes of the T-S signals measured in the two manners are more evident than the difference in shape (Figure 3). The amplitudes of the T-S signals of both microwave transitions are considerably larger than those of the corresponding (T-S)(α) signals. For the $|D| - |E|$ transition (Figure 3A) the ratio of the amplitudes of the T-S to T-S(α) spectrum is 1.3 at 808 nm, 1.5 at 818 nm, and 1.3 at 900 nm. In the $|D| + |E|$ transition (Figure 3B) the ratios are 1.9 at 808 nm, 1.3 at 818 nm, and 1.7 at 900 nm. For the $|D| - |E|$ transition the integrated area of the P(–) band from 860 to 930 nm in the T-S spectrum is 1.3 times larger than the corresponding area in the (T-S)(α) spectrum. For the $|D| + |E|$ transition, this ratio is 1.7.

The relative intensity of the P(–) band in the absorption, T-S, and LD(T-S) spectra is important when analyzing the *Rb. sphaeroides* data via exciton calculations. The LD(T-S) spectra are correctly scaled to the (T-S)(α) in refs 7 and 9 with the dichroic ratio of the P(–) band. The oscillator strength of the P(–) band of the absorption spectrum should be scaled to that of the T-S spectrum because in this band only $S_1 \leftarrow S_0$ absorption without the presence of a triplet occurs.⁷ However, in refs 7 and 9 the areas of the P(–) bands of the absorption spectrum and the (T-S)(α) spectrum are set equal. The authors consider the negative part of the (T-S)(α) spectrum to be equal to the singlet absorption spectrum. This procedure incorrectly scales (cf. eq 16) the dipolar strength of the P(–) band for *Rb. sphaeroides* in the absorption spectrum to 77% and 59% of its value for the $|D| - |E|$ and $|D| + |E|$ transitions, respectively. The decrease in oscillator strength in the P(–) band leads to lower values of μ_S and $T\mu_S$ (cf. eq 12).

The angles α are determined by calculating the ratio of the amplitudes of an isolated band in the LD(T-S) and (T-S)(α) spectra at low microwave powers. In Figure 5, the amplitude of the band at 900 nm in the LD(T-S) spectrum (dots) is shown versus the corresponding amplitude in the (T-S)(α) spectrum as a function of microwave power, for both the $|D| - |E|$ and $|D| + |E|$ transitions of the BChl dimer (data from ref 7). A

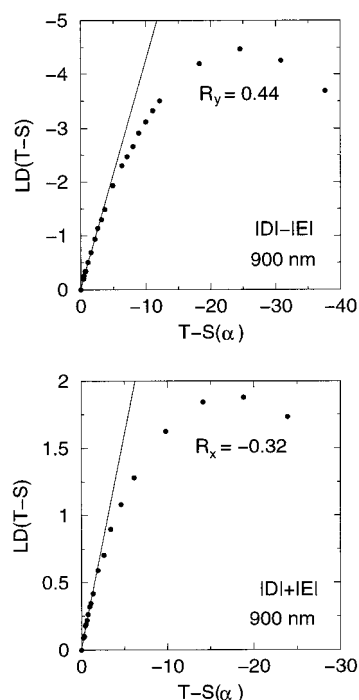


Figure 5. Amplitude at 900 nm of the LD(T-S) to the T-S(α) spectrum at various microwave powers (≈ 0.01 –50 mW at the microwave source) for reaction centers of *Rb. sphaeroides* R26 (data from ref 7). In (A) and (B) the microwave frequencies were set to the $|D| - |E|$ transition (467 MHz) and $|D| + |E|$ (658 MHz) transition, respectively. A solid line connects points measured at low microwave powers.

straight line connects the points measured at low microwave powers. Since the P(–) band is well separated from the other bands, the angle α_S is determined from the slope R of this straight line (see Figure 5). This slope is known as the dichroic ratio and is given by²¹

$$R = \frac{\text{LD(T-S)}}{\text{T-S}(\alpha)} = \frac{\Delta A_V - \Delta A_H}{\Delta A_V + \Delta A_H} = \frac{3 \cos^2 \alpha - 1}{3 + \cos^2 \alpha} \quad (18)$$

The angles α determined from the isolated bands are relatively accurate, as are those derived from a Gaussian fit of only the T-S(α) and the LD(T-S) spectra. However, if these two spectra are fit *simultaneously* with an incorrectly scaled absorbance spectrum, the resulting angles may be inaccurate. Furthermore, the definition of R as the ratio of the LD(T-S) to the T-S signal^{7,8,21} should be discontinued since it leads to misconceptions. The dichroic ratio R should be defined as the ratio of the LD(T-S) to the T-S(α) signal measured under nonsaturating conditions.

Exciton simulations of ADMR-detected T-S(α) and LD(T-S) spectra have been performed in ref 12 on the FMO complex of *Pr. aestuarii*. In Figure 6A the T-S(α) spectrum (solid line) and the T-S spectrum (dotted line), reconstructed from the data of ref 12 and eq 17, are shown for the $|D| - |E|$ transition of the triplet-carrying BChl. In Figure 6B the corresponding LD(T-S) spectrum (solid line) measured as $(\Delta A_V - \Delta A_H)$ is shown. The ratio of LD(T-S) to the T-S(α) signals for the $|D| - |E|$ transition is especially large for the well-isolated 827 nm band (approximately 0.5), indicating that the measurements were done under nonsaturating conditions.

Also shown in Figure 6A is the T-S spectrum scaled (dashed line) to maximize overlap with the T-S(α) spectrum. The scaled T-S spectrum is less intense than the T-S(α) spectrum

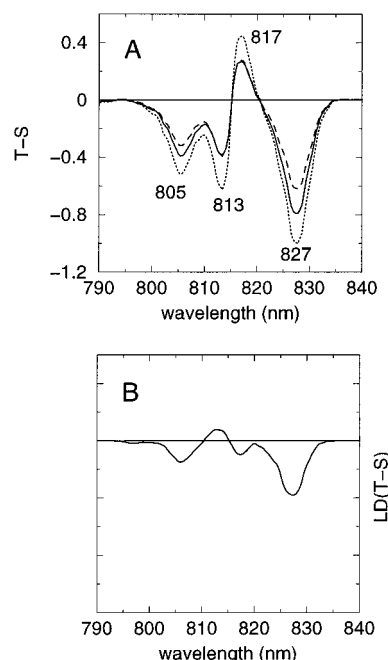


Figure 6. Microwave-induced T-S(α) absorbance difference spectra (solid line), the T-S absorbance difference spectra (dotted line), and a scaled T-S spectrum (dashed line) of the FMO complex of *Pr. aestuarii* shown in (A) for the $|D| - |E|$ transition (464 MHz). The LD(T-S) spectrum measured as $(\Delta A_V - \Delta A_H)$ (solid line) is shown in (B) for the $|D| - |E|$ transition (464 MHz). The y-axis labels for the T-S spectra also hold for the LD(T-S) spectra. Data are from ref 8.

in the 803–810 nm and in the 820–835 nm regions. The 820–835 nm region of the two spectra overlap for this scaling. The T-S spectrum is more intense than the T-S(α) spectrum. The ratio of the amplitudes of the T-S to the T-S(α) spectra are 1.3 at 805 nm, 1.6 at 813 nm, 1.6 at 817 nm, and 1.3 at 827 nm.

In order to simultaneously fit all spectra (absorption, T-S, LD(T-S)) the intensity of the spectra needs to be normalized. In ref 12 the LD(T-S) spectra are correctly scaled to the T-S(α) spectra by using the dichroic ratio of the well-isolated 827 nm band, a step which acknowledges that the T-S(α) spectra are dependent on α . However, the intensity of the triplet-carrying bacteriochlorophyll in the T-S(α) spectrum was set equal to the intensity of the corresponding band in the absorption spectrum. In this procedure it was incorrectly assumed that the T-S spectra were free of α -angular dependency, and the dipolar strength of the 827 nm band was scaled to 79% (based on integration from 821 to 833 nm) of its value. The scaling will result in a lower value of μ_S and, due to the simultaneous fitting procedure, changes in T_{μ_S} , T_{α_S} , and α_S , as well. For example, we used the same scaling as in ref 12 for the absorption, T-S(α), and LD(T-S) spectra in the $|D| - |E|$ transition. We then fit the absorption band at 827 nm with $|\mu|^2 \rho(\omega_\lambda)$ and the T-S(α) and LD(T-S) spectra with eqs 12 and 14, respectively. With this procedure we obtained an angle α of 0° instead of the experimentally found 10° .

4. Conclusion

ADMR-detected T-S spectroscopy is a well-established technique. Care should be taken when analyzing the spectra. This especially concerns their correct identification as either T-S or T-S(α) spectra. When not performed correctly, the analysis results in incorrect values for the angles α between

the optical and microwave transition moments and for the dipole moments of the optical transitions.

References and Notes

- (1) Maki, A. H. In *Biological Magnetic Resonance*; Berliner, L. J., Reuben, J., Eds.; Plenum Press: New York, 1984; Vol. 6, p 187.
- (2) Hoff, A. J. In *Advanced EPR: Applications in Biology and Biochemistry*; Hoff, A. J., Ed.; Elsevier: Amsterdam, 1989; p 633.
- (3) Aust, V.; Angerhofer, A.; Ullrich, J.; Von Schütz, J. U.; Wolf, H. C. *Chem. Phys. Lett.* **1991**, *181*, 213.
- (4) Lous, E. J.; Hoff, A. J. *Proc. Natl. Acad. Sci. U.S.A.* **1987**, *84*, 6147.
- (5) Carbonera, D.; Giacometti, G.; Agostini, G. *FEBS Lett.* **1994**, *343*, 200.
- (6) Hartwich, G.; Scheer, H.; Aust, V.; Angerhofer, A. *Biophys. Biochim. Acta* **1995**, *1230*, 97.
- (7) Vrieze, J.; Hoff, A. J. *Biochim. Biophys. Acta* **1996**, *1276*, 210.
- (8) Louwe, R. J. W.; Vrieze, J.; Aartsma, T. J.; Hoff, A. J. *J. Phys. Chem. B* **1997**, *101*, 11273.
- (9) Knapp, E. W.; Scherer, P. O. J.; Fischer, S. F. *Biochim. Biophys. Acta* **1986**, *852*, 295.
- (10) Scherer, P. O. J.; Fischer, S. F. *Biochim. Biophys. Acta* **1987**, *891*, 157.
- (11) Scherer, P. O. J.; Fischer, S. F. *Chem. Phys. Lett.* **1987**, *137*, 32.
- (12) Louwe, R. J. W.; Vrieze, J.; Aartsma, T. J.; Hoff, A. J. *J. Phys. Chem. B* **1997**, *101*, 11280.
- (13) Owen, G. M.; Hoff, A. J. *J. Phys. Chem. B* **1999**, *103*, 10789.
- (14) Den Blanken, H. J.; Hoff, A. J. *Biochim. Biophys. Acta* **1982**, *681*, 365.
- (15) Schellman, J. A. *Chem. Rev.* **1975**, *75*, 323.
- (16) Kirmaier, C.; Holten, D.; Parson, W. W. *Biochim. Biophys. Acta* **1985**, *810*, 33.
- (17) Thompson, M. A.; Zerner, M. C.; Fajer, J. J. *J. Phys. Chem.* **1991**, *95*, 5693.
- (18) Breton, J. In *The Photosynthetic Bacterial Reaction Center: Structure and Dynamics*; Breton, J., Verméglio, A., Eds.; Plenum Press: New York, 1988; p 59.
- (19) Parson, W. W.; Warshel, A. J. *Am. Chem. Soc.* **1987**, *109*, 6152.
- (20) Lous, E. J. Ph.D. Thesis, Leiden University, Leiden, The Netherlands, 1988.
- (21) Meiburg, R. F. Ph.D. Thesis, Leiden University, Leiden, The Netherlands, 1985.